



DOI: 10.18721/JPM.13308  
УДК 532.5.013.13:532.526

## THE EFFECT OF LARGE-SCALE DISTURBANCES ON THE LAMINAR-TURBULENT TRANSITION IN A FREE-CONVECTIVE LAYER ON A VERTICAL SURFACE: AN EXPERIMENTAL STUDY

*Yu.S. Chumakov, E.F. Khrapunov, A.D. Malykh*

Peter the Great St. Petersburg Polytechnic University, St. Petersburg, Russian Federation

The results of an experimental study of a free convective boundary layer on a vertical heated surface are presented in this paper. Particular attention has been paid to investigation of the laminar-turbulent transition zone and determination of the zone boundaries. The main goal of the present work was to find the opportunity of the transition processes' control by using various large-scale obstacles located in the region of the laminar section of the boundary layer. A vertical aluminum plate 90 cm wide and 4.95 m high served as a free-convection flow generator. Based on the obtained results, it is safe to state that there is a possibility of a significant reduction in the length of the transition zone through the use of large-scale obstacles. This way permits the beginning of the region with developed turbulent heat transfer to be moved nearer to the front edge of the surface. Thus, these obstacles can be considered as passive elements for controlling the heat transfer intensity.

**Keywords:** natural convection, laminar-turbulent transition, heat transfer, natural convective boundary layer, experimental study

**Citation:** Chumakov Yu.S., Khrapunov E.F., Malykh A.D., The effect of large-scale disturbances on the laminar-turbulent transition in a free-convective layer on a vertical surface: an experimental study, St. Petersburg Polytechnical State University Journal. Physics and Mathematics. 13 (3) (2020) 93–101. DOI: 10.18721/JPM.13308

This is an open access article under the CC BY-NC 4.0 license (<https://creativecommons.org/licenses/by-nc/4.0/>)

## ЭКСПЕРИМЕНТАЛЬНОЕ ИССЛЕДОВАНИЕ ВЛИЯНИЯ КРУПНОМАСШТАБНЫХ ВОЗМУЩЕНИЙ НА ЛАМИНАРНО-ТУРБУЛЕНТНЫЙ ПЕРЕХОД В СВОБОДНОКОНВЕКТИВНОМ СЛОЕ НА ВЕРТИКАЛЬНОЙ ПОВЕРХНОСТИ

*Ю.С. Чумаков, Е.Ф. Храпунов, А.Д. Малых*

Санкт-Петербургский политехнический университет Петра Великого,  
Санкт-Петербург, Российская Федерация

В работе описываются результаты экспериментального исследования свободноконвективного пограничного слоя на вертикальной нагретой поверхности, причем особое внимание уделяется изучению зоны ламинарно-турбулентного перехода, определению границ этой зоны. Основная цель данного исследования — найти возможность управления процессами перехода, воздействуя на них различными крупномасштабными препятствиями, расположенными в области ламинарного участка пограничного слоя. Генератором свободноконвективного потока служила вертикальная алюминиевая пластина шириной 90 см и высотой 4,95 м. На основании полученных результатов можно с уверенностью утверждать, что с помощью крупномасштабных препятствий удастся заметно сократить протяженность зоны перехода и тем самым приблизить начало области с развитым турбулентным теплообменом к передней кромке поверхности. Таким образом, препятствия можно рассматривать как пассивные элементы для управления интенсивностью теплообмена.

**Ключевые слова:** свободная конвекция, ламинарно-турбулентный переход, теплообмен, свободноконвективный пограничный слой, экспериментальное исследование

**Ссылка при цитировании:** Чумаков Ю.С., Храпунов Е.Ф., Малых А.Д. Экспериментальное исследование влияния крупномасштабных возмущений на ламинарно-турбулентный переход в свободноконвективном слое на вертикальной поверхности // Научно-технические ведомости СПбГПУ. Физико-математические науки. 2020. Т. 3 № .13. С. 108–118. DOI: 10.18721/JPM.13308

Статья открытого доступа, распространяемая по лицензии CC BY-NC 4.0 (<https://creativecommons.org/licenses/by-nc/4.0/>)

## Introduction

Numerous studies have considered the development of forced convective boundary layers under the influence of different types of external factors. In particular, it was discovered that external disturbances with low intensity have little effect on the transient processes in the boundary layer. Large-scale three-dimensional obstacles (the so-called macro-roughness elements) placed in the laminar region of the boundary layer can serve to achieve sharp acceleration in the development of unsteady processes and transition to turbulence in the near-wall layer. Such macro-roughnesses are widely used to control the laminar-turbulent transition (LTT) in forced convective flows, for example, for obtaining relatively thick boundary layers in landscape wind tunnels to simulate the flow of the surface boundary layer around different objects [1].

While sufficient experience in numerical and physical simulation of methods for controlling LTT with macroroughness elements has been accumulated for forced convective flows, very few studies deal with free convective flows. For example, the results of direct numerical simulation of turbulence developing in a free-convective layer in the wake of macro-obstacles have been given so far only in [2], and we were unable to uncover any results of physical simulation. However, it is natural to assume that the LTT region (whose length in the absence of disturbances is two to three times greater than the length of the laminar region) can be substantially reduced by generating the appropriate conditions for sudden ‘trigger’ excitation of turbulence in the boundary layer [3–5]. In turn, the length of the turbulent heat transfer region and therefore the intensity of heat transfer in general can be increased by reducing the length of the LTT region.

This paper reports on the results of experimental study of the LTT region in a free-convective boundary layer near a vertical heated plate with a cross-row of large-scale 3D obstacles disturbing the initially laminar layer arranged on the surface. The measurement data obtained in for a flat plate are also given for comparison.

## Problem statement

Our main goal consisted in exploring the possibility of controlling the transition processes in a free-convective boundary layer using different large-scale obstacles located in the laminar region of the boundary layer.

Two types of plates with a thickness of 8 mm were used as obstacles: with a rectangular section of  $32 \times 18$  mm, and with a trapezoidal section with a height of 18 mm, where the lower base was 32 mm long and the upper one 16 mm long. The obstacles were glued to the plate across the vertical axis at a distance of 200 mm from the lower edge of the plate with a pitch of 32 mm. Fig. 1 shows a schematic representation of the plates, and a photograph of the obstacles installed on the heated surface.

The height of the obstacles  $H$  was chosen by estimating the thickness of the undisturbed laminar boundary layer in the region where the obstacle was supposed to be installed. The thickness of the boundary layer  $\delta$  (m) can be estimated by the well-known semi-empirical formula [6] for air:

$$\delta = 4.23 \left( \frac{\nu^2 \cdot X}{g \cdot \beta \cdot \Delta T \cdot \text{Pr}} \right)^{1/4}, \quad (1)$$

where  $\nu$ ,  $\text{m}^2/\text{s}$ , is the kinematic coefficient of viscosity;  $X$ , m, is the axial coordinate;  $g$ ,  $\text{m}/\text{s}^2$ , is the acceleration of gravity;  $\beta$ ,  $\text{K}^{-1}$ , is the coefficient of thermal expansion of the medium;  $\Delta T = T_w - T_\infty$ , K, is the characteristic temperature difference ( $T_w$ ,  $T_\infty$  are the temperature of the plate surface and the temperature at the outer edge of the boundary layer, respectively); Pr is the Prandtl number.

When  $X = 200$  mm, the layer thickness is  $\delta = 13$  mm, and the ratio of the obstacle height  $H$  to the layer thickness is  $H/\delta = 1.4$ , i.e., the obstacle protrudes slightly beyond the boundary layer. Notably, all temperature-dependent parameters in this formula and further in the text depend on the thermal conditions described below, including the characteristic temperature difference  $\Delta T$ .

### Brief description of the experimental test bench and measurement methods

Free convective flow was generated by a vertical aluminum plate with a width of 90 cm and a height of 4.95 m. A total of 25 heaters (not shown in Fig. 1) were mounted on the back side of the plate; they were controlled by an electronic system capable of maintaining the given temperature conditions for a long time. Different laws for heating the surface along its height and, in particular, constant surface temperature were simulated by setting a specific regime for each of the 25 sections. Because the plate was very high, all three flow regimes, i.e., laminar, transitional, and fully developed turbulent could be simulated up to the Grashof number  $Gr = 4.5 \cdot 10^{11}$ . A detailed description of the experimental testbed is given in [5, 7].

Averaged and fluctuation components of the temperature and the axial component of the velocity vector were measured. All measurements were made using a resistance thermometer and a hot-wire anemometer (TA).

The measuring probe consists of two sensors where tungsten wires with a diameter of  $5 \mu\text{m}$  and a length of 3–4 mm are used as sensitive elements. The wires of both sensors are located parallel to each other, spaced 2 mm apart, and parallel to the surface; the lower sensor (upstream with respect to the flow) measures the current temperature, and the upper sensor (after processing of the initial data) measures the current velocity.

It is known that if the velocity in nonisothermal flow is measured by thermal anemometry, the anemometer readings should be interpreted taking into account the temperature

values. The given flow is characterized by low mean velocities and a high level of fluctuations, so the current velocities are typically measured by the method of thermal compensation by mean temperature, which can yield inaccurate velocity measurements.

We used the thermal compensation method described in [8] in this study. Without dwelling on a detailed description of this method, let us only note that unlike other methods of thermal compensation by mean temperature, the TA reading corresponding to the current velocity at a given point in space is interpreted taking into account the current temperature at the same point.

All measurements were carried out at a constant surface temperature  $T_w = 60 \pm 0.5^\circ\text{C}$ , while the air temperature at the outer edge of the boundary layer  $T_\infty$  varied from 24 to  $26^\circ\text{C}$  during the entire experimental period.

A coordinate device was used to move the sensor within the boundary layer, providing an accuracy of movement of about 1 mm along the vertical (axial) coordinate  $X$  and of about  $1 \mu\text{m}$  along the coordinate  $Y$  normal to the surface (i.e., across the boundary layer); movement along the normal coordinate was carried out remotely, in automatic mode. The coordinate system used is shown in Fig. 1.

Flow parameters were measured fully automatically in each section of the boundary layer.

The measurement sequence is described as follows.

1. Probe is moved (with an accuracy of 1 mm) in the selected section along the axial coordinate  $X$  (see Fig. 1).
2. The probe is automatically brought to the surface until touching it.

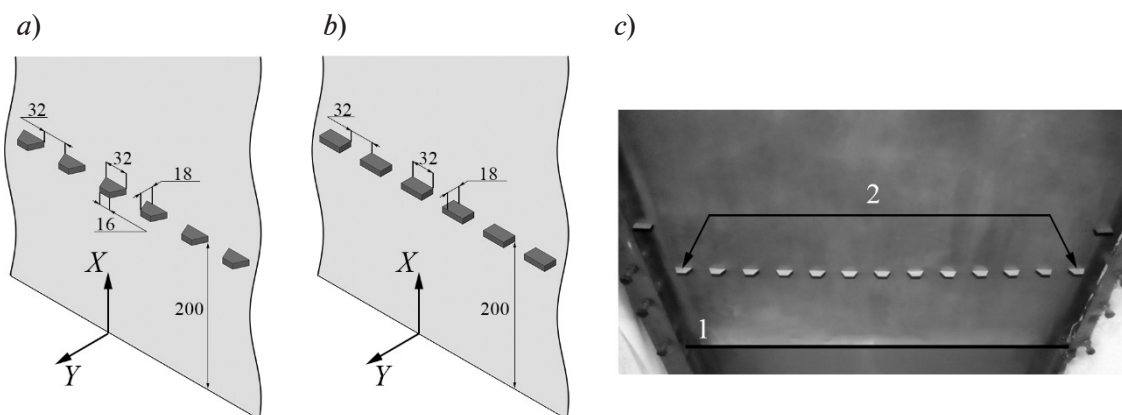


Fig. 1. Schemes of trapezoidal (a) and rectangular (b) elements; photograph of heated plate (c) showing its face (1) and trapezoidal elements serving as obstacles (2). The distances in the figure are given in mm

3. After movement stops, the probe is moved away from the surface at a distance of 0.6 mm (with an accuracy of 1 μm).

4. The probe is ready to perform measurements in automatic mode along the normal coordinate  $Y$  with the given pitch.

5. Readings are taken from both sensors of the probe at each point almost simultaneously (with an interval of  $10^{-5}$  s); such measurements are repeated with a given frequency (100 Hz). Typically, 2,000 samples of reading pairs were taken; thus, the time of one measurement was 20 s.

After appropriate data processing, we obtained a record of the current values of temperature and velocity at a given point. Then, after performing the averaging operation, we calculated the mean values of velocity, temperature and fluctuation intensity.

### Comparative analysis of the results

The influence of obstacles on the laminar-turbulent transition was studied by comparing the results of measuring the averaged and fluctuation characteristics of temperature and velocity fields in the near-wall region of the boundary layer. The results of a detailed study on the free-convection boundary layer without disturbances are given in [3–5,9,10]. These studies describe the main characteristics of LTT, in particular, the local peaks appearing for mean velocity and its fluctuation intensity, as well as the intensity of temperature fluctuations at the end of the transition region.

It was assumed in earlier studies that the axial coordinate  $X$  of the maximum values of fluctuation intensity can be considered the beginning of a fully developed turbulent boundary layer. However, analysis of the fields of current values of temperature and velocity indicates that the intermittency factor in the region of maximum values of fluctuation intensity is approximately 0.65–0.75, which only points towards increasing intensity of the transition process. In fact, it can be assumed that the LTT has ended and the flow in the boundary layer has passed into a fully developed turbulent regime only downstream relative to the coordinate of the maximum, when the fluctuation intensity slightly decreases and almost does not change with an increase in the axial coordinate. The intermittency factor reaches 0.80–0.95 in this region.

The main conclusions obtained in previous studies [3–5,9,10], served as the basis for selecting criteria for assessing the length of

the LTT region and detecting the beginning of the fully developed turbulent regime in a free-convection boundary layer.

All results for the flow without disturbances introduced (case B1) are shown by circles in the graphs below; the results for rectangular obstacles (case B2), by squares, and for the results of trapezoidal obstacles (case B3) by triangles.

The maximum values of the following dimensionless characteristics of the flow were analyzed:

temperature fluctuation intensities,  $IT_m$ ,

$$IT_m = \left( \sqrt{t^2} / \Delta T \right)_{\max}, \quad (2)$$

where  $T_m$ , K, is the maximum temperature in a given section of the boundary layer;  $t$ , K, is the fluctuation component of the current temperature;

velocity fluctuation intensities,  $IU_m$ ,

$$IU_m = \left( \sqrt{u^2} / U_b \right)_{\max}, \quad (3)$$

where  $U_m$ , m/s, is the maximum velocity in a given section of the boundary layer;  $u$ , m/s, is the fluctuation component of the current axial velocity;  $U_b$ , m/s, is the buoyancy velocity, determined by the relation  $U_b = (g\beta\Delta T\nu)^{1/3}$ ;

dimensionless mean velocity  $U_m/U_b$  in the given section along the coordinate  $X$ .

It was not our intention to measure the full distributions of the characteristics of the boundary layer. Only the near-wall part of the distribution was measured, and this was sufficient to objectively assess the maximum values of the given characteristics in this section along the axial coordinate  $X$ .

Fig. 2 shows the distributions of the maximum values of temperature fluctuation intensity  $IT_m$  with respect to the local Grashof number, as well as along the dimensional coordinate  $X$  for the three given cases of obstacles. The thermophysical properties of air for calculating the Grashof number were taken at a mean temperature equal to  $(T_w + T_\infty)/2$ . The exception was the value of the thermal expansion coefficient, which was estimated at external temperature. The Grashof number is determined by the relation

$$Gr_x = \frac{g \cdot \beta \cdot \Delta T \cdot X^3}{\nu^2}. \quad (4)$$

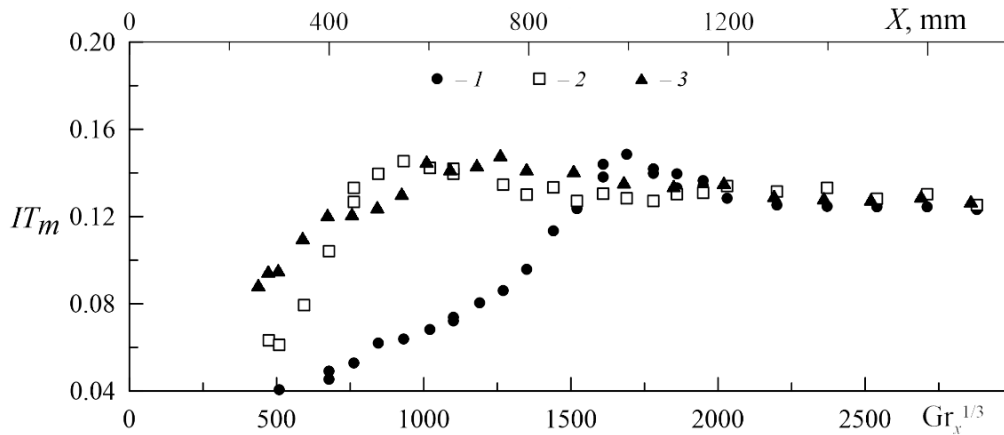


Fig. 2. Maximum values of temperature fluctuation intensity  $IT_m$  in the section across the layer depending on local Grashof number  $Gr_x$  for three cases of obstacles (the curve numbers correspond to the case numbers)

Analysis of the data obtained for case B1 made it possible to discover the following features:

- a smooth increase in the fluctuation intensity  $IT_m$  up to the maximum value at  $X \approx 1000$  mm,  $Gr_x \approx 4.9 \cdot 10^9$ ;

- a slight subsequent decrease in  $IT_m$ ; starting from  $X \approx 1200$  mm ( $Gr_x \approx 8.4 \cdot 10^9$ ), the values of  $IT_m$  practically do not change.

Analysis of the results obtained for cases B2 and B3 allows us to draw the following conclusions:

- the growth rate of  $IT_m$  is about 20% higher for case B2, than the corresponding velocity for case B3 up to  $X \approx 450$  mm ( $Gr_x \approx 4.4 \cdot 10^8$ ). Then, starting from  $X \approx 500$  mm ( $Gr_x \approx 6.1 \cdot 10^8$ ), the fluctuation values  $IT_m$  observed for

- B3 sharply increase and reach the maximum value at  $X \approx 550$  mm ( $Gr_x \approx 8.1 \cdot 10^8$ ). In turn, the fluctuations  $IT_m$  reach their maximum value only at  $X \approx 750$  mm ( $Gr_x \approx 2.0 \cdot 10^9$ ) for B2;

- the values of the temperature fluctuation intensity for B2 and B3 approach each other with a further increase in the values of the coordinate  $X$  (local Grashof number), and, starting from  $X \approx 1200$  mm ( $Gr_x \approx 8.4 \cdot 10^9$ ) are combined with  $IT_m$  for B1, reaching an almost constant value.

Fig. 3 shows the distributions of the maximum values of velocity fluctuations  $IU_m$  along the plate for the three given cases. The following was established from analysis of the data presented:

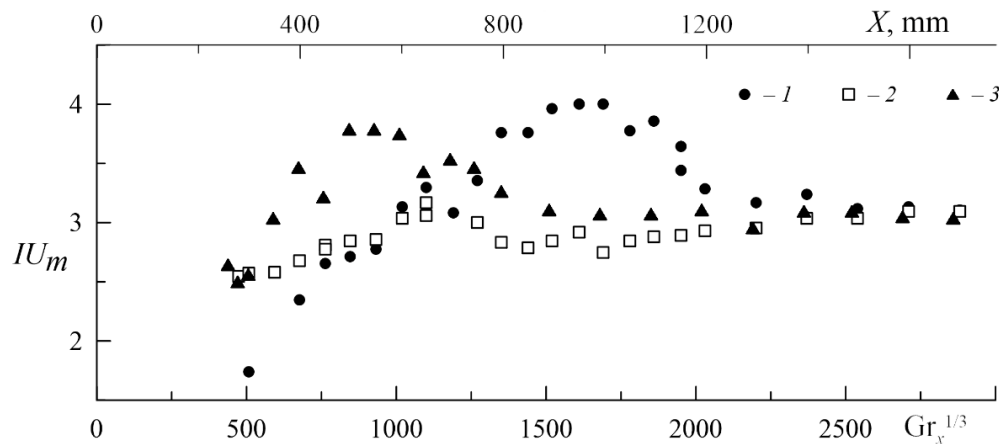


Fig. 3. Maximum values of velocity fluctuation intensity  $IU_m$  in the section across the layer depending on local Grashof number  $Gr_x$  for three cases of obstacles (the curve numbers correspond to the case numbers)

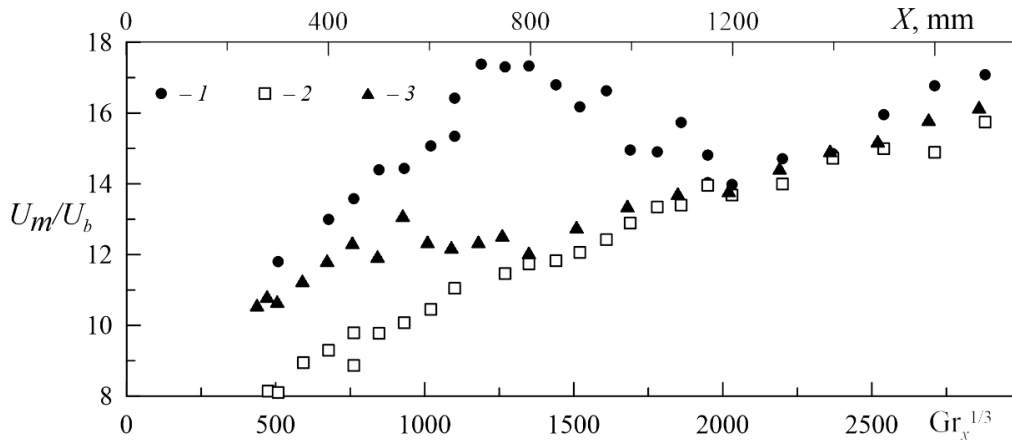


Fig. 4. Maximum values of dimensionless mean velocity  $U_m/U_b$  in the section across the layer depending on local Grashof number  $Gr_x$  for three cases of obstacles (the curve numbers correspond to the case numbers)

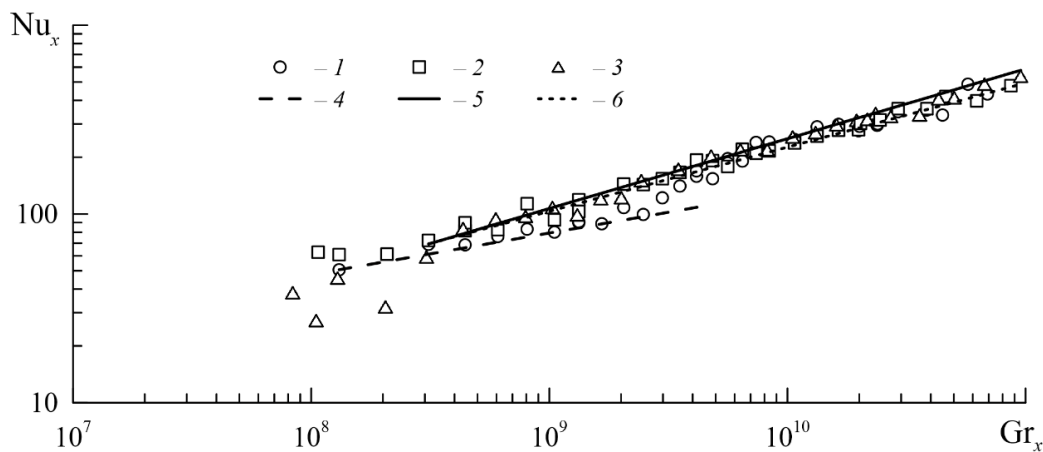


Fig. 5. Dependences of Nusselt number on Grashof number for three cases of obstacles (the first numbers of the curves correspond to the numbers of the cases);

segments of curves 4–6 are additionally shown:

(4)  $Nu_x^{lam} = 0.83 Gr_x^{0.22}$ ; (5)  $Nu_x = 0.05 Gr_x^{0.37}$ ; (6)  $Nu_x = 0.09 Gr_x^{0.34}$

starting from  $X \approx 300$  mm ( $Gr_x \approx 1.3 \cdot 10^8$ ), the fluctuation intensity  $IU_m$  for both cases with disturbances (B2 and B3) considerably exceeds the fluctuation intensity  $IU_m$  for the case without disturbances. Moreover, a rapid increase in the intensity  $IU_m$  is observed for B2, and the maximum values of  $IU_m$  are reached at  $X = 500$  mm ( $Gr_x \approx 6.1 \cdot 10^8$ );

the intensities  $IU_m$  increase almost equally up to  $X \approx 650$  mm ( $Gr_x \approx 1.3 \cdot 10^9$ ) for B3 and B1, then  $IU_m$  for B3 begins to decrease, and the fluctuation intensity for B1 increases, reaching a maximum value at  $X \approx 950$  mm ( $Gr_x \approx 4.2 \cdot 10^9$ );

the intensities  $IU_m$  approach each other for all three cases with a further increase

in the values of the coordinate  $X$  (local Grashof number), reaching identical values at  $X \approx 1400$  mm ( $Gr_x \approx 1.3 \cdot 10^{10}$ ).

Fig. 4 shows the distributions of the maximum values of the dimensionless mean velocity  $U_m/U_b$  with respect to the Grashof number. The following was established from analysis of the data presented:

the values of the maximum velocity  $U_m/U_b$  at the beginning of the boundary layer ( $X \approx 300$  mm or  $Gr_x \approx 1.3 \cdot 10^8$ ) for the three cases were distributed in accordance with resistances to the developing flow from the disturbances (obstacles). For example, case B3 has the greatest resistance, for which the value of velocity  $U_m/U_b$  increases monotonically



throughout the entire section observed. At the same time, the velocities  $U_m/U_b$  for cases B2 and B1 increase almost identically up to the coordinate  $X \approx 400$  mm ( $Gr_x \approx 3.1 \cdot 10^8$ ). After that the velocity  $U_m/U_b$  for case B2 still deviates from the values for B1, starting to slow down and merging with the curve for B3 at a distance  $X \approx 900$  mm ( $Gr_x \approx 3.5 \cdot 10^9$ ).

as expected, the velocity  $U_m/U_b$  for B1 steadily reaches the maximum value at  $X \approx 850$  mm ( $Gr_x \approx 2.3 \cdot 10^9$ ) and then, slowly decreasing, merges with the curves for the two other cases at  $X \approx 1200$  mm ( $Gr_x \approx 8.4 \cdot 10^9$ ).

Before we can analyze the results obtained for heat transfer, let us briefly describe the procedure for determining the local heat transfer coefficient  $\alpha$  ( $W/(m^2 \cdot K)$ ) and, ultimately, the Nusselt number  $Nu_x$ , expressed as

$$Nu_x = \frac{\alpha \cdot X}{\lambda}, \quad (5)$$

where  $\lambda$ ,  $W/(m \cdot K)$ , is the thermal conductivity.

The procedure is based on the technique proposed in [3–5]. According to this technique, there is a thin heat-conducting layer near the wall, where the distribution of the averaged temperature linearly depends on the normal coordinate  $Y$ . Based on this, the heat flux  $q_w$  from the surface can be represented in the following form:

$$q_w = -\lambda \cdot \left( \frac{\partial T}{\partial Y} \right) \Big|_w = \alpha \cdot \Delta T. \quad (6)$$

Consequently, the local heat transfer coefficient  $\alpha$  can be easily calculated if the derivative is determined graphically from the experimental temperature distribution.

The degree to which the disturbances influence the process of transition from

laminar to turbulent flow is well observed from the variation in heat transfer in this region. Fig. 5 shows the dependences of the Nusselt number  $Nu_x$  on the local Grashof number  $Gr_x$  for the case without disturbances (B1) and two cases with disturbances (B2 and B3).

Two regions are distinctly observed for B1: laminar and turbulent regions of the boundary layer with the corresponding laws of heat transfer:

$$Nu_x^{lam} = 0.83 Gr_x^{0.22}; \quad Nu_x^{turb} = 0.07 Gr_x^{0.35}.$$

Additionally, notice the fairly extended LTT region ( $Gr_x \in (2 - 10) \cdot 10^9$ ). A complete absence of a laminar region is observed for both cases upstream after the obstacles. Moreover, a region with the laws of heat transfer characteristic for a turbulent flow regime begins almost immediately after the obstacles. For example, this ratio is  $Nu_x = 0.05 \cdot Gr_x^{0.37}$  for the case B2, and  $Nu_x = 0.09 \cdot Gr_x^{0.34}$  for the case B3.

## Conclusion

Based on the data presented in the paper, we can claim with confidence that large-scale obstacles can be used to substantially reduce the length of the transition region in free-convective boundary layers, moving the beginning of the region with fully developed turbulent heat transfer closer to the leading edge of the streamlined surface. In terms of practical application, obstacles of this kind can serve as passive elements for controlling the intensity of heat transfer.

The study was financially supported by a Russian Science Foundation grant (project no. 18-19-00082).

## REFERENCES

1. Irwin H.P.A.H., The design of spires for wind simulation, *J. Wind Engin. Ind. Aerod.* 7 (3) (1981) 361–366.
2. Smirnov E.M., Abramov A.G., Smirnovsky A.A., Smirnov P.E., Numerical simulation of turbulence arising in the free convection boundary layer after across row of rectangular obstacles, *J. Phys., Conf. Ser.* 1128 (2018) 012090.
3. Tsuji T., Nagano Y., Characteristics of a turbulent natural convection boundary layer along a vertical flat plate, *Int. J. Heat Mass Transfer.* 31 (8) (1988) 1723–1734.
4. Chumakov Yr.S., Kuzmitsky V.A., Surface shear stress and heat flux measurements on a vertical heated plate under free convection heat transfer // *Russian Journal of Engineering Thermophysics.* 8 (1–4) (1998) 1–15.
5. Kuzmitskii V.A., Chumakov Yu.S., Analysis of characteristics of flow under conditions of laminar-to-turbulent transition in a free-convection boundary layer, *High Temperature.* 37 (2) (1999) 217–223.
6. Popov I.A., *Gidrodinamika i teploobmen vneshnikh i vnutrennikh svobodnokonvektivnykh vertikalnykh techeniy s intensifikatsiyey*

[Hydrodynamics and heat transfer of external and internal vertical free-convective flows with intensification], Tsentr Innovatsionnykh Tekhnologiy, Kazan, 2007 (in Russian).

7. **Chumakov Yu.S., Levchenya A.M., Khrapunov E.F.**, An experimental study of the flow in the area of influence of a cylinder immersed in the free convective boundary layer on a vertical surface, St. Petersburg State Polytechnical University Journal. Physics and Mathematics. 13 (1) (2020) 66–77.

8. **Kuzmitskii V.A., Chumakov Yu.S.**, Facility

for static calibration of a hot-wire anemometer at low velocities in a nonisothermal air medium, High Temperature. 33 (1) (1995) 109–113.

9. **Nikol'skaya S.B., Chumakov Yu.S.**, Experimental investigation of pulsation motion in a free-convection boundary layer, High Temperature. 38 (2) (2000) 231–237.

10. **Tsuji T., Nagano Y.**, Turbulence measurements in a natural convection boundary layer along a vertical flat plate, Int. J. Heat Mass Transfer. 31 (10) (1988) 2101–2111.

Received 25.06.2020, accepted 27.07.2020.

## THE AUTHORS

### **CHUMAKOV Yuriy S.**

*Peter the Great St. Petersburg Polytechnic University*

29 Politechnicheskaya St., St. Petersburg, 195251, Russian Federation

chumakov@yahoo.com

### **KHRAPUNOV Evgeniy F.**

*Peter the Great St. Petersburg Polytechnic University*

29 Politechnicheskaya St., St. Petersburg, 195251, Russian Federation

hrapunov.evgenii@yandex.ru

### **MALYKH Anastasiya D.**

*Peter the Great St. Petersburg Polytechnic University*

29 Politechnicheskaya St., St. Petersburg, 195251, Russian Federation

anfaterna@yandex.ru

## СПИСОК ЛИТЕРАТУРЫ

1. **Irwin H.P.A.H.** The design of spires for wind simulation // Journal of Wind Engineering & Industrial Aerodynamics. 1981. Vol. 7. No. 3. Pp. 361–366.

2. **Smirnov E.M., Abramov A.G., Smirnovsky A.A., Smirnov P.E.** Numerical simulation of turbulence arising in the free convection boundary layer after across row of rectangular obstacles // Journal of Physics: Conference Series. 2018. Vol. 1128. P. 012090.

3. **Tsuji T., Nagano Y.** Characteristics of a turbulent natural convection boundary layer along a vertical flat plate // International Journal of Heat and Mass Transfer. 1988. Vol. 31. No. 8. Pp. 1723–1734.

4. **Chumakov Yu.S., Kuzmitsky V.A.** Surface shear stress and heat flux measurements on a vertical heated plate under free convection heat transfer // Russian Journal of Engineering Thermophysics (Институт теплофизики им. С.С. Кутателадзе Сибирского отделения РАН). 1998. Vol. 8. No. 1–4. Pp. 1–15.

5. **Кузьмицкий В.А., Чумаков Ю.С.** Анализ

характеристик течения при ламинарно-турбулентном переходе в свободноконвективном пограничном слое // Теплофизика высоких температур 1999. Т. 37. № 2. С. 239–246.

6. **Попов И.А.** Гидродинамика и теплообмен внешних и внутренних свободноконвективных вертикальных течений с интенсификацией. Интенсификация теплообмена: монография. Под общ. ред. Ю.Ф. Гортышова. Казань: Центр инновационных технологий, 2007. 326 с.

7. **Чумаков Ю.С., Левченя А.М., Храпунов Е.Ф.** Экспериментальное исследование течения в зоне влияния цилиндра, погруженного в свободноконвективный пограничный слой на вертикальной поверхности // Научно-технические ведомости СПбГПУ. Физико-математические науки. 2020. Т. 13. № 1. С. 66–77.

8. **Кузьмицкий В.А., Чумаков Ю.С.** Установка для калибровки термоанемометра при малых скоростях в неизотермической воздушной среде // Теплофизика высоких температур. 1995. Т. 33. № 1. С. 116–120.



9. **Никольская С.Б., Чумаков Ю.С.** Экспериментальное исследование пульсационного движения в свободноконвективном пограничном слое // Теплофизика высоких температур. 2000. Т. 38. № 2. С. 249–256.

10. **Tsuji T., Nagano Y.** Turbulence measurements in a natural convection boundary layer along a vertical flat plate // International Journal of Heat and Mass Transfer. 1988. Vol. 31. No. 10. Pp. 2101–2111.

*Статья поступила в редакцию 25.06.2020, принята к публикации 27.07.2020.*

### **СВЕДЕНИЯ ОБ АВТОРАХ**

**ЧУМАКОВ Юрий Сергеевич** – доктор физико-математических наук, профессор Высшей школы прикладной математики и вычислительной физики Санкт-Петербургского политехнического университета Петра Великого, Санкт-Петербург, Российская Федерация.

195251, Российская Федерация, г. Санкт-Петербург, Политехническая ул., 29  
chumakov@yahoo.com

**ХРАПУНОВ Евгений Федорович** – аспирант Высшей школы прикладной математики и вычислительной физики Санкт-Петербургского политехнического университета Петра Великого, Санкт-Петербург, Российская Федерация.

195251, Российская Федерация, г. Санкт-Петербург, Политехническая ул., 29  
hrapunov.evgenii@yandex.ru

**МАЛЫХ Анастасия Денисовна** – студентка магистратуры Высшей школы прикладной математики и вычислительной физики Санкт-Петербургского политехнического университета Петра Великого, Санкт-Петербург, Российская Федерация.

195251, Российская Федерация, г. Санкт-Петербург, Политехническая ул., 29  
anfatneva@yandex.ru